SCANNING VOL. 30, 65–77 (2008)

Morphology and Amine Accessibility of (3-Aminopropyl) Triethoxysilane Films on Glass Surfaces

WEI WANG and MARK. W. VAUGHN

Department of Chemical Engineering, Texas Tech University, Lubbock, Texas, USA

Summary: 3-Aminopropyl) triethoxysilane (APTES) is commonly used to functionalize glass substrates because it can form an amine-reactive film that is tightly attached to the surface. In this study, we investigated the morphology and chemical reactivity of APTES films prepared on glass substrates using common deposition techniques. Films were prepared using concentrated vapor-phase deposition, dilute vapor-phase deposition, anhydrous organic-phase deposition and aqueous-phase deposition. All films were annealed, or cured, at 150 °C. The morphology of the films was quantified by fluorescence and by atomic force microscopy (AFM). The optical equivalent of the AFM images was computed and then used to directly compare optical and AFM images. Reactive amine density was determined by a picric acid assay and by a method that employed *N*-succinimidyl 3-[2-pyridyldithio]-propionamido (SPDP) cross-linked rhodamine. Fluorescence and AFM images showed that silane films prepared from dilute vapor-phase and aqueous-phase deposition were more uniform and had fewer domains than those deposited by the other methods. The ratio of picric acid-accessible amino groups to SPDP cross-linked rhodamine-accessible groups varied with the preparation method, suggesting reactant size-dependent difference in amine accessibility. We found a larger number of accessible amino groups on films prepared by vapor-phase deposition than on those prepared from solution deposition. The dilute vapor-phase deposition technique produced relatively few domains, and it should be a good choice for bioconjugation applications. There were appreciable differences in the films produced by each method. We suggest that these differences originate from differences in film rearrangement during annealing. SCANNING 30: 65–77, 2008.

Address for reprints: M. W. Vaughn, Department of Chemical Engineering, Texas Tech University, Lubbock, TX 79409-4121, USA e-mail: mark.vaughn@ttu.edu

Received 26 Sep 2007; Accepted with revision 07 Jan 2008

Key words: bioconjugation, atomic force microscopy, fluorescence microscopy, APTES, optical imaging, image analysis, silanol

Introduction

Silanization of solid surfaces with APTES is widely used to prepare substrates for applications using immobilized proteins and to prepare selective absorbents or organic/inorganic hybrid materials (Kurth and Bein, 1995; Hu *et al*., 1996; Frey *et al*., 1997; Joos *et al*., 1997; Szabo *et al*., 1998; Gyorvary *et al*., 1999; Falsey *et al*., 2001; LeProust *et al*., 2001; Kim and Abbott, 2002; Matsumoto *et al*., 2002; Ek *et al*., 2003; Etienne and Walcarius, 2003; Jin *et al*., 2003; Miyazaki *et al*., 2003; Wang *et al*., 2003; Vaidya and Norton, 2004; Crampton *et al*., 2005; Chen *et al*., 2006; Enders *et al*., 2007; Martin *et al*., 2007; Yu *et al*., 2007). Chemically adsorbed silane on an inorganic surface provides a platform for further chemical reactions through an amine or other functional group opposite to the silane. Hence, macromolecules like protein and DNA can be fixed onto the platform by linking to the functional group.

Typically, a silane-modified surface is prepared by depositing a silane compound onto a silica, glass or aluminum oxide substrate to form a thin film of grafted material. Silanes can be deposited from either solution or vapor phases (Peanasky *et al*., 1995; Moon *et al*., 1996; Ek *et al*., 2003). The film can then be annealed, or cured, at an elevated temperature to form cross-links between the substrate and silane molecules (Heiney *et al*., 2000; Falsey *et al*., 2001; Sun *et al*., 2002).

Silane film morphology can affect the accessibility of reactive groups, thereby altering the degree of immobilization and possibly the properties of the subsequently immobilized molecules (Chechik and Stirling, 1998; Heiney *et al*., 2000; Zhuang *et al*., 2000). A better understanding of the relationship between morphology, amino group accessibility and the deposition method could lead to more effective silane application. Although silane films prepared by different methods might be expected to differ in morphology and

in the accessibility of the amino groups, few studies have examined this relationship. In what follows, we examine the structure of amino-terminated silane films at the micro and submicroscale using fluorescence microscopy and AFM, augmented by amine group chemical availability measurements. Direct comparison between AFM measurements of surface topology and fluorescently labeled features is enabled by converting the AFM topology into an "optical equivalent" image. This image approximates the image that would be obtained if the optical features of the film resulted from surface topography only.

Macroscale properties of silane films have been characterized by use of Fourier transform infrared (FTIR) spectroscopy (Kessel and Granick, 1991; Kanan *et al*., 2002), X-ray photoelectron spectroscopy (Moon *et al*., 1997; Allen *et al*., 2005; Crampton *et al*., 2005; Chen *et al*., 2006; Metwalli *et al*., 2006; Martin *et al*., 2007), UV-vis spectrophotometry (Moon *et al*., 1996, 1997), ellipsometry (Kurth and Bein, 1995; Moon *et al*., 1996, 1997), and quartz-crystal microbalance measurements(Kurth and Bein, 1995). These methods have provided essential insight into film properties but cannot describe the distribution of available amino groups or the microscale morphology of the film. The AFM has been used to provide nanoscale morphology of silane films but not the accessibility and distribution of amino groups.

Some silanes, such as octadecyltrichlorosilane (OTS) can form smooth, monolayer-like films on SiO_2, (Tidswell *et al*., 1991; Legrange *et al*., 1993; Peanasky *et al*., 1995; Wang and Lieberman, 2003; Koga *et al*., 2005) although the type of film formed depends on the experimental conditions (Legrange *et al*., 1993; McGovern *et al*., 1994; Peters *et al*., 2002; Fan *et al*., 2003; Rozlosnik *et al*., 2003; Koga *et al*., 2005). Particularly important is the amount of water in the system (Legrange *et al*., 1993; McGovern *et al*., 1994; Ulman, 1996; Peters *et al*., 2002; Foisner *et al*., 2003; Wang and Lieberman, 2003) and the nature of the solvent (McGovern *et al*., 1994; Fan *et al*., 2003; Rozlosnik *et al*., 2003). (3-Aminopropyl) triethoxysilane was originally thought to form an ordered monolayer with adjacent silanes bound by Si–O–Si bonds, (Waddell *et al*., 1981; Kurth and Bein, 1993; Moon *et al*., 1996). However the APTES–SiO_2 interaction is complicated. The film formed can be multilayered (Kang and Blum, 1991; Moon *et al*., 1997), and the properties of the layer are strongly influenced by several major factors. These factors include silane bond-length mismatch in the assembled 2D film, (Stevens, 1999) water on the substrate surface or in solution, (White and Tripp, 2000; Zhang and Srinivasan, 2004; Howarter and Youngblood, 2006) silane concentration, (Kang and Blum, 1991; Etienne and Walcarius, 2003; Zhang and Srinivasan, 2004; Howarter and Youngblood, 2006) reaction time for film formation (Moon *et al*., 1996, 1997; Heiney *et al*., 2000; Howarter and Youngblood, 2006), reaction temperature, (Howarter and Youngblood, 2006) and amine–glass interactions (Vandenberg *et al*., 1991; White and Tripp, 2000; Kanan *et al*., 2002). An important factor in the behavior of APTES is its propensity to form intermolecular siloxane crosslinks (Crampton *et al*., 2005; Howarter and Youngblood, 2006, 2007).

Atomic force microscopy has been used in a number of morphological studies of silane films. Studies have focused on factors that affect film formation, evolution and structure, (Sun *et al*., 2002; Benitez *et al*., 2003; Rozlosnik *et al*., 2003; Zhang and Srinivasan, 2004; Allen *et al*., 2005; Jung *et al*., 2005; Howarter and Youngblood, 2006) film growth mechanisms, (Simon *et al*., 2002; Foisner *et al*., 2003; Wang and Lieberman, 2003; Crampton *et al*., 2005; Metwalli *et al*., 2006) and mechanical properties (Nakagawa *et al*., 1994; Xiao *et al*., 1995).

Allen *et al*. (2005) studied self-assembled 3-amino propyl trimethoxysilane (APTMS) films by the use of XPS, SIMS and AFM. In their work, AFM was used to measure nanoscale surface homogeneity and three-dimensional assembled film features. They were interested in whether the film was continuous or composed of island structures. Their AFM images indicated that the APTMS film was homogeneous, without pits or defects. Benitez *et al*. (2003) investigated octadecylamine multilayers on mica with AFM. They found that multilayer films were formed, exposing terraces with alternating frictional and wear properties due to methyl and amino group terminations. They proposed the growth mechanism as micellar formation in the ethanol solution and subsequent deposition onto the mica. Howarter and Youngblood (2006) used AFM to study the effect of reaction temperature, solution concentration and reaction time on the structure and morphology of APTES films. They found three basic morphologies: smooth thin films, smooth thick films and roughened thick films. Jung *et al*. (2005) used AFM to examine the vapor-phase self-assembled monolayer and found that the vapor-phase treated substrates had fewer aggregates of the silane molecules on the surface. Rozlosnik *et al*. (2003) used AFM to examine the effect of solvents and concentration on the formation of OTS monolayers. They found that OTS in heptane could form a fully covered monolayer on hydrophilic silicon oxide, whereas OTS in dodecane results in multilayer films. Sun *et al*. (2002) studied the structural evolution of octyltriethoxysilane (OTE) films on glass surfaces by the use of pulsed-force mode AFM. They found that the films formed at room temperature were flat and featureless, but the samples annealed at 145 °C showed formation of "islands". The size and number of these islands increased with the annealing time.

Crampton *et al*. (2005) considered factors affecting the functionalization of mica with aminosilanes. Their

contact mode AFM scratching experiments showed that the monolayer structure of silane film existed when the relative humidity (RH) was below 25% and the bilayer structure film existed when the RH was above 25%. The discontinuity at 25% RH appeared to be correlated with the appearance of liquid water on the surface. Both structures were found to bind DNA. Crampton *et al*. (2005) also investigated the structural changes of the two layer types after annealing at 150 °C. They found that the structural changes that occurred during annealing could prevent DNA from binding to silane-modified mica. Wang and Lieberman (2003) used AFM and XPS to investigate OTS monolayer formation. They found that film formation from a dry solution of OTS in Isopar-G occurred through a "patch expansion" process that terminated once a single monolayer was formed. However, when a small amount of water was present in the solution, OTS formed plate-like islands on the surface. Octadecyltrichlorosilane films formed in wet solutions covered the surface much faster than those formed in dry solutions. Additionally, they found that wet-solution films were not monolayers and that longer deposition time resulted in increased roughness. Aqueous and anhydrous deposition of APTES was investigated by Simon *et al*. (2002) who found that the most stable films were formed by deposition from anhydrous solution. Foisner *et al*. (2003) studied the growth of alkylsiloxane monolayers from various concentrations in toluene by the use of tapping mode AFM and ellipsometry. They found that irregular rough films with a maximum surface coverage of 70% could be formed from a high concentration of OTS solution.

Nakagawa *et al*. (1994) used AFM to investigate the topography of OTS on mica surfaces. They found that the film could be imaged repeatedly without being damaged when the scanning force was set at about 1 nN. They also found that the film had pinholes that ranged in size from several nanometers to about 100 nm. Xiao *et al*. (1995) determined the structure and mechanical stability of OTE monolayers on mica with AFM. They found that the films could be removed with sharp AFM tips by applying a load above 10 nN. They concluded that the mechanical strength of the films formed by OTE was due to inter-siloxane cross-linking rather than to chemical bonding to the mica substrate.

The purpose of this paper is to compare the morphology of APTES films prepared by commonly used methods and to evaluate the chemical accessibility of the amine groups on those films. Fluorescence techniques provided microscopic and macroscopic surface density information: macroscopic information through the intensity distribution and microscopic information through the concentration dependence of intensity. The accessibility of the silane amino groups was evaluated by assays using amine-reactive compounds: picric acid and fluorescently tagged SPDP. Atomic force microscopy was used to characterize film topography.

Materials and Methods

Chemicals

N-Succinimidyl-3-(2-pyridyldithio) propionate was purchased from Pierce Biotechnology (Rockford IL). APTES, rhodamine-B-isothiocyanate (RITC), DL-1,4-dithiothreitol (DTT), cystine, cysteine and high-performance liquid chromatography (HPLC)-grade water, were purchased from either Acros (Fisher Scientific, Houston) or Sigma-Aldrich (St. Louis).

Substrate Preparation

Borosilicate glass microscope cover slides (24 mm × 40 mm) (Fisher Premium #1 coverslips, Fisher Scientific, Houston) were cleaned with 100 °C piranha solution (a mixture of 2/3 concentrated H_2SO4 and 1/3 30% H_2O_2) for 6 h, then washed and stored in deionized water. All slides were used within 1 week of cleaning. Prior to use, slides were dried in a 120 °C oven for 2 h, then cooled to room temperature.

Silane Film Preparation

Silane films were prepared by methods described elsewhere with slight modifications (Wikstrom *et al*., 1988; Falsey *et al*., 2001).

Method 1: concentrated vapor-phase deposition. Two clean slides were put inside a clean, horizontal 200 mL glass bottle that contained 50 µL of APTES. The bottle was sealed and placed in a 150 °C oven for 20 h.

Method 2: dilute vapor-phase deposition. A solution of 0.1 mL APTES in 10 mL dry toluene was prepared. Two clean slides were put inside a clean, horizontal 200 mL glass bottle that contained 50 µL of the APTES–toluene solution. The bottle was sealed and placed in a 150 °C oven for 20 h.

Method 3: organic-phase deposition. Toluene was dried by adding five grams anhydrous Na_2SO_4 to 50 mL toluene for 10 min. (3-Aminopropyl) triethoxysilane was added to the dry toluene to make a 2% APTES–toluene solution. Clean glass slides were immersed into the solution and reacted at room temperature for 2 h on a rocking mixer. The slides were then removed, washed with toluene and dichloromethane and placed in bottle. The bottle was sealed and placed in a 150 °C oven for 20 h.

Method 4: aqueous-phase deposition. Clean slides were soaked in a 2% APTES solution for 2 h on a rocking mixer. The slides were removed, washed with deionized water, then placed in a bottle. The bottle was sealed and placed in a 150 °C oven for 20 h.

Amine Density

Amino group density of the APTES film was characterized by two methods.

Method 1: the picric acid method. We followed the procedure described by Gisin (1972). Briefly, two APTES coated glass slides were neutralized with 5% (v/v) diisopropylethylamine in dichloromethane for 6 min, then washed with dichloromethane for 2 min. The slides were treated with 0.1 M picric acid for 10 min and washed five times with dichloromethane for 2 min each time. The picrate was eluted with diisopropylethylamine solution for 6 min. The solution absorption at 358 nm was measured spectrophotometrically. The concentration of the amino groups in the solution was obtained by comparing the absorption at 358 nm of the unknown solution with that of a standard picrate solution.

Method 2: the SPDP/RITC method. The reaction scheme is shown in Figure 1. This method was developed in order to investigate the amine groups accessible to bioconjugation, especially bioconjugation of peptides, oligonucleotides and other bulky groups. The procedure is modified from a SPDP protocol given by Hermanson (1999). The APTES coated glass slides were activated by immersing in a SPDP–DMSO (dimethyl sulfoxide) solution (5 mg/10 mL) for 3 h. Unreacted SPDP was removed by washing the slide with DMSO. The cystine linker was attached by reacting in 20 mL of 0.1 M cystine in HPLC grade water for 3 h. The slides were then immersed in RITC solution in 40 mM phosphate buffer solution for 3 h. Finally, the slides were treated with a 0.1 M DTT solution for 3 h to reduce the cystine disulfide bond and release the rhodamine from the surface. The concentration of the amino groups in the solution was obtained by comparing the final solution fluorescent intensity to that of a standard RITC solution prepared from an equal molar ratio RITC–SPDP–cysteine mixture diluted with 0.1 M DTT.

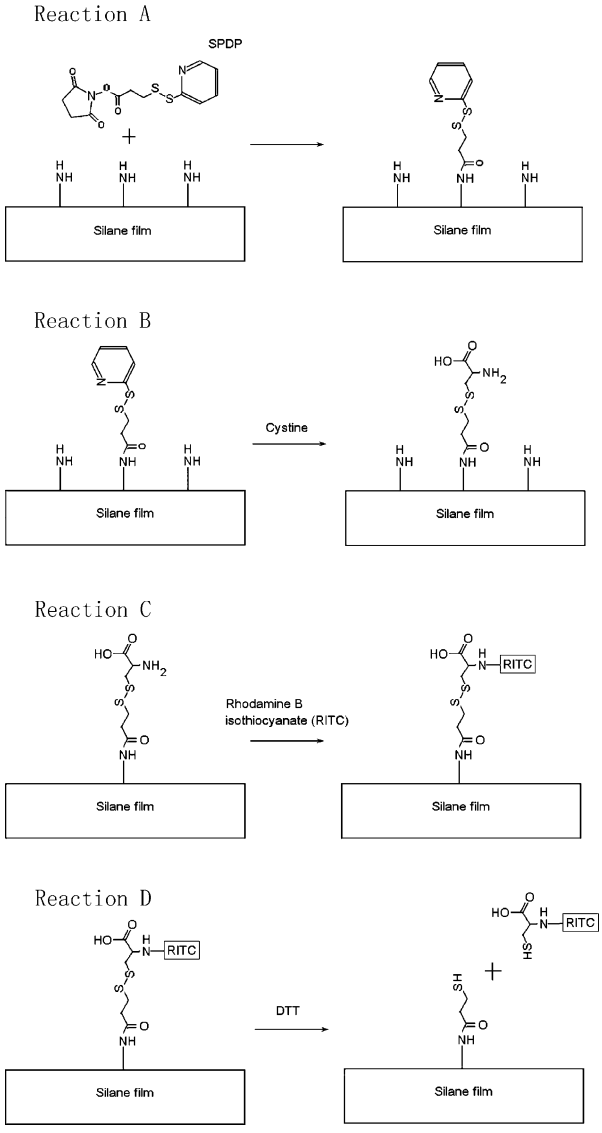

Fig 1. Reaction scheme for determining accessible amine density using *N*-succinimidyl-3-(2-pyridyldithio) propionate (SPDP) cross-linked rhodamine to react with amine groups on a (3-aminopropyl)triethoxysilane film. After attachment and visualization, rhodamine can be released for quantification by reducing the linker disufide bond.

Fluorescence Microscopy

All optical images were taken with an Olympus IX71 fluorescence microscope through a 40 × 0.6 NA long-working distance lens using an Olympus Q-Color 3 CCD camera. Photomicrographs were taken using a 100 W mercury arc light source with a standard fluorescein (488 nm excitation/510 nm emission) filter set or a standard rhodamine (540 excitation/605 emission) filter set (Chroma, Rockingham, VT). Grayscale images were obtained from the color CCD photographs from the green channel (510 nm emission) or red channel (605 emission) using NIH ImageJ (Rasband, 1997–2007).

Atomic Force Microscopy

The AFM images of silane films were taken with a PSIA XE-100 Scanning Probe Microscope. The sample was mounted on an XY scanner and scanned in contact mode. Triangular Veeco MLCT-AUHW Microlever Probes with nominal constant of 0.01–0.03 N/m were used for imaging. The X, Y and Z voltage were set low to obtain a lateral resolution of 0.76 nm and a vertical resolution of 0.125 nm. The scanning force was set between 1 and 10 nN and the scanning rate was set between 0.7 and 0.9 Hz. Each sample was scanned

several times to get a representative image. The image size was typically 5 by 5 μm^2. All images represented a 1024 by 1024 matrix of values, resampled to 256 by 256 pixels.

Optical Equivalent Atomic Force Microscopy Images

The optical equivalent of the AFM images was obtained by projecting each AFM pixel as a point-source of light, the intensity of which was proportional to its height.

A point-source of light is transformed to an Airy disk as a result of the finite wavelength of light and diffraction-limited optics. The first root of the Airy disk is located at $r_{\mathrm{Airy}} = 0.61\lambda/NA$, where NA is the numerical aperture of the objective and λ is the wavelength of the light. (Keller, 2006) For the objective used for our images, $r_{\mathrm{Airy}} \cong 0.56$ µm. The normalized Airy disk intensity can be expressed as

$$I(r) = [2\mathrm{J}_1(1.22\pi r/r_{\mathrm{Airy}})/(1.22\pi r/r_{\mathrm{Airy}})]^2 \qquad (1)$$

where J_1 is a Bessel function of the first kind, order one. (see, e.g. Born and Wolf, 1980, p. 396) Numerically, this is well approximated (integrated intensities differ by less than 0.01%) by the Gaussian function $I_G(r)$=exp$(-(r/r_{\mathrm{Airy}})^2/2\sigma^2)$, where r is the radial coordinate of the diffraction-limited spot and $\sigma = 0.4301$ in r/r_{Airy} units.

The AFM height data were convolved with the point-spread function $I_G(r)$ by applying a standard "Gaussian blur" filter to the acquired image. Many graphical software packages including the free, cross-platform packages ImageJ (Rasband, 1997–2007) and the Gnu Image Manipulation Program, GIMP (http://www.gimp.org) implement this filter. A region sampled at $s = d/n$ µm/pixel, where d is distance (the image size) and n is the number of pixels required a Gaussian filter with a pixel "width" given by its standard deviation, $\sigma_G = 0.4301 r_{Airy} n/d$. For example, the 5 µm × 5 µm images below were sampled at 256 × 256 pixels with $d = 5$ mm and $n = 256$ pixels. Their equivalent optical image was obtained by applying a Gaussian filter with a "radius" σ_G of 12 pixels. Optical and optical equivalent AFM images were compared after the intensity of the equivalent image was scaled so that mean intensity equaled that of the corresponding microscope image and the contrast adjusted so that the image variance equaled that of the optical microscope image.

Results and Discussion

Intrinsic Fluorescence of APTES Films

All four silanization methods produced natively fluorescent films. Since a clean glass substrate is completely dark when observed through a fluorescence microscope, the fluorescence comes from the film. Figure 2 shows images of the intrinsic fluorescence of APTES films prepared using the four deposition methods. All samples were annealed, or cured, at the same conditions: 20 h at 150 °C. Many silanization procedures do not call for annealing. (see Joos *et al*., 1997; Simon *et al*., 2002; Howarter and Youngblood, 2006, for example). However, if the film is not annealed, the APTES should be considered absorbed to the hydrated glass surface, rather than covalently bound (Waddell *et al*., 1981; Zhang and Srinivasan, 2004). Nonannealed silane films can differ significantly in structure from annealed films, (Sun *et al*., 2002; Zhang and Srinivasan, 2004, Crampton *et al*., 2005) because of flow, diffusion and dewetting during the annealing process (Fan *et al*., 2003).

Figure 2, shows that the fluorescent intensity depends on the film deposition method. For a monolayer APTES film, there should be no fluorescence. The fluorescence appears to be a result of a three-dimensional silane structure on the glass substrate (Bekiari and Lianos, 1998; Uchida *et al*., 2000). Therefore, the fluorescent intensity should increase with the film thickness and indicates a multilayer film. The film prepared by concentrated vapor-phase deposition Figure 2(A), was the most fluorescent, whereas the film prepared by aqueous-phase deposition, Figure 2(D), was the least

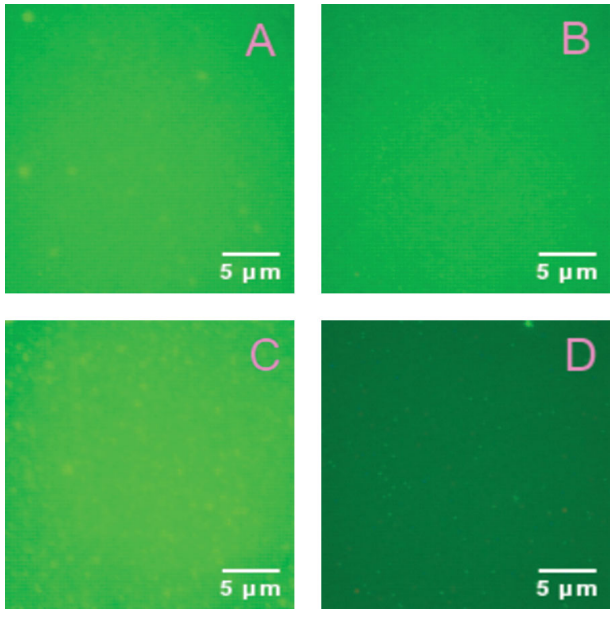

Fig 2. Photomicrographs of the intrinsic fluorescence of annealed (3-aminopropyl) triethoxysilane surfaces produced by different deposition methods: (A) concentrated vapor-phase deposition, (B) dilute vapor-phase deposition, (C) organic-phase deposition, (D) aqueous-phase deposition. Uniform intensity suggests a uniform layer. The exposure time of images A–D are 3, 5, 5 and 8 s, respectively, chosen to give similar average intensity. The scale bar is 5 µm long. This figure is available in colour online at www.interscience.wiley.com/SCA.

fluorescent. These films should be the thickest and the thinest, respectively. Figure 2(A) and (C) show a number of micrometer-sized bright regions that we suggest are islands or domains formed during the annealing process, (Crampton *et al*., 2006). The bright intrinsic fluorescence of these regions suggests that the domains have a well-defined three-dimensional structure.

Atomic Force Microscopy Images of APTES Films

Although bright regions in the fluorescent images suggest the presence of islands or domains, fluorescent images provide only two-dimensional microscale information. Therefore, the surface topography of these features was quantified with AFM. Figure 3 shows typical images of the surface topography. Like Figure 2, these images suggest that domains exist in films produced by all four deposition methods. The height and the number of the domains differed according to preparation method: domains in the dilute vapor-phase deposited films (Figure 3(B)) were smaller in lateral extent and spaced more regularly than those in liquid deposited films. Domains similar to those of Figure 3(B) have been reported for films of OTE (Sun *et al*., 2002) where they appeared to be induced by annealing. Although the OTE film domains (Sun *et al*., 2002) were similar in size to those measured here, their surface number density was higher and their interdomain spacing was less regular than the domains we found for the dilute vapor-phase deposited films.

Figure 3 indicates that the APTES films prepared by vapor-phase deposition methods had a domain height of 5–10 nm, whereas the domain height was 2 nm for the aqueous-phase deposition method and 50 nm for the organic-phase deposition method. These values refer to the heights of the feature, not the thickness of the underlying film. The film surface prepared using aqueous-phase deposition was comparatively flat and featureless, consistent with the fluorescence microscope images Figures 2 and 4.

RITC-labeled APTES Films

To determine the microscale morphology of the amine-reactive sites, the APTES films were labeled with RITC, which reacted with the amine groups of the

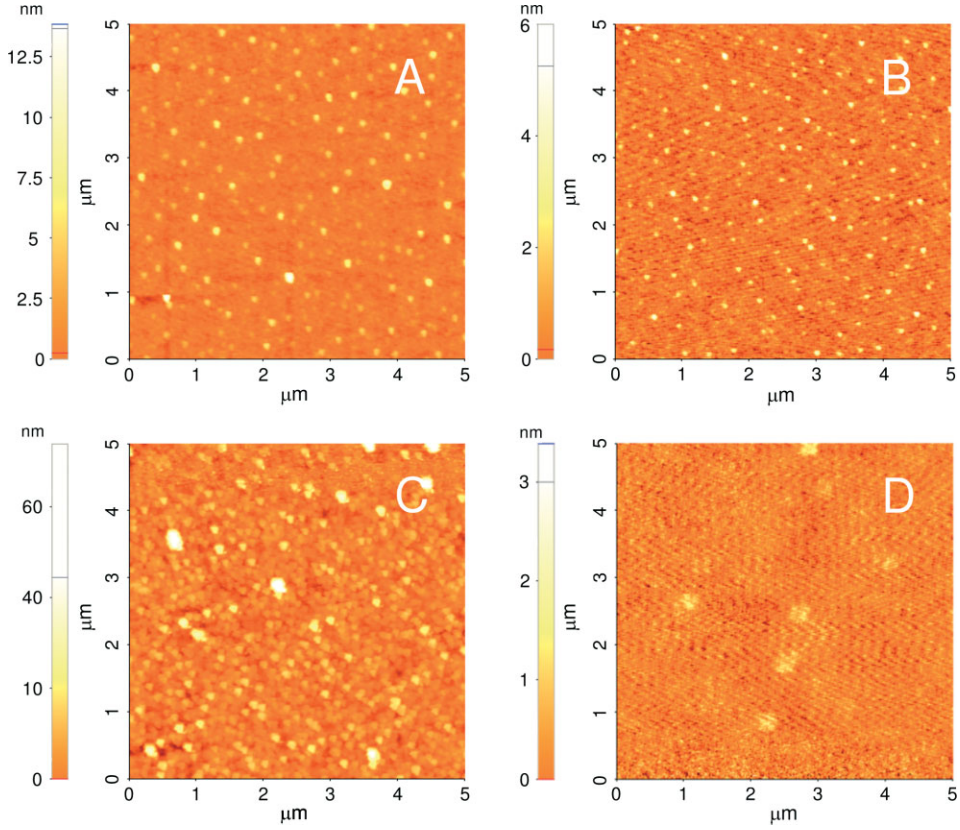

Fig 3. Atomic force microscope image of annealed (3-aminopropyl)triethoxysilane surfaces produced from different deposition method: (A) concentrated vapor-phase deposition, (B) dilute vapor-phase deposition, (C) organic-phase deposition, (D) aqueous-phase deposition. The ordered islands in the vapor-phase deposition are probably formed during annealing. Each image is 5 µm square. This figure is available in colour online at www.interscience.wiley.com/SCA.

APTES film by forming a thiourea bond. (Hermanson, 1999) After RITC attachment, the fluorescence was more intense than that of the unlabeled film. Figure 4 shows images of typical RITC-labeled APTES films. As in Figure 2, bright regions are prevalent on slides prepared from the concentrated vapor-phase deposition and organic-phase deposition methods. Figure 4 suggests that the microscale RITC-accessible morphology is different from that responsible for the intrinsic fluorescence of Figure 2, since the RITC-labeled fluorescence of the solution-deposited films was less uniform than the intrinsic fluorescence.

Features responsible for bright regions in the unlabeled samples, Figure 2 are not necessarily responsible for the bright regions of RITC-labeled samples of Figure 4. There is no assurance that high intrinsic fluorescent intensity correlates with a high density of accessible amine groups. High intrinsic intensity could indicate a film that is thick and dense in APTES, but whose amine groups inaccessible.

Even if bright intrinsic fluorescence correlated with highly accessible amine-groups, self-quenching from resonance energy transfer between attached rhodamine groups could reduce the intensity so a quantitative relationship between the two optical images would not exist. Self-quenching is important for fluorophores that are separated by distances on the order of the Forster distance, which is about 5.5 nm for the rhodamine–rhodamine pair (Macdonald, 1990). The images in Figure 4 suggest that self-quenching probably plays a role, since the exposure times show an opposite trend to that of the intrinsic fluorescence. For the RITC-tagged fluorescence, the image exposure times of Figure 4 were 1.5, 1, 0.6 and 0.5 s, for concentrated and dilute vapor-phase, organic- and aqueous-phase deposition, respectively. The thick concentrated vapor film had the least intense RITC fluorescence.

Figure 5 shows the intensity histograms for the optical images of Figures 2 and 4. These histograms

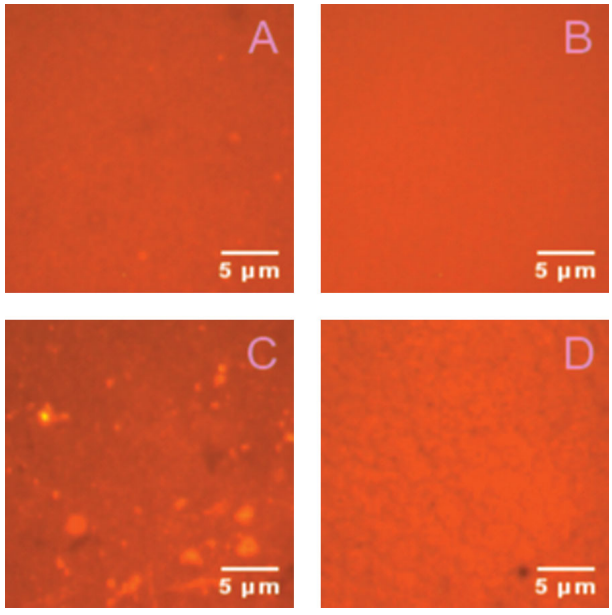

Fig 4. Photomicrographs of the of rhodamine isothiocyanate-tagged annealed (3-aminopropyl) triethoxysilane fluorescence surfaces produced from different deposition methods: (A) concentrated vapor-phase deposition, (B) dilute vapor-phase deposition, (C) organic-phase deposition, (D) aqueous-phase deposition. Because the amine groups may be buried and the rhodamine isothiocyanate can self-quench, the domains indicated by intensity differ from those of Figure 2. The exposure times of the films in panels A–D was 1.5, 1, 0.6 and 0.5 s, respectively. This figure is available in colour online at www.interscience.wiley.com/SCA.

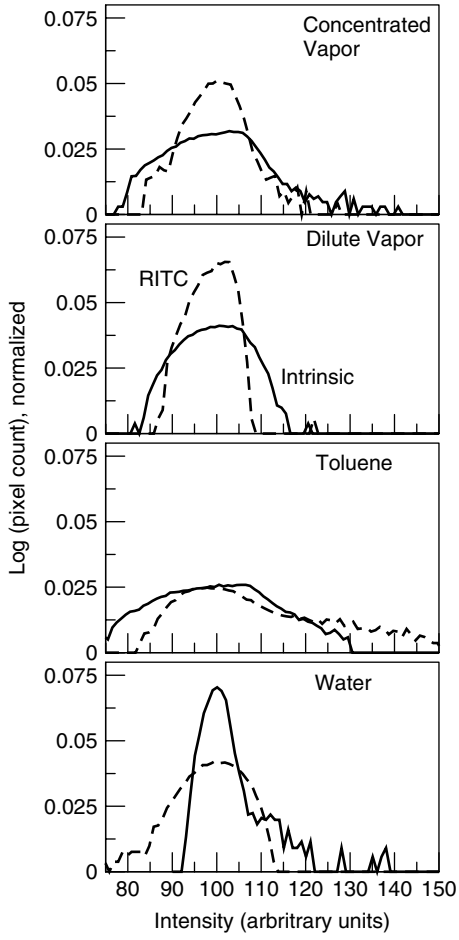

Fig 5. Microscale film heterogeneity as measured by intensity variation. A histogram of fluorescent intensity for concentrated vapor-phase deposition; dilute vapor-phase deposition; organic-phase deposition; and aqueous-phase deposition. The solid line is the intrinsic (3-aminopropyl) triethoxysilane film fluorescence and the dashed line is the rhodamine-tagged fluorescence. The curves are the log of the binned intensity (gray value, scaled 0–255) with the average intensity scaled to 100 and the count normalized to unit area under each curve. A perfectly uniform layer would be indicated by a single sharp peak at 100.

provide a measure of microscale morphology for the APTES films. They show the pixel count, binned from 0 (no light) to 255 (maximum brightness), with the mean intensity normalized to 100 and the count normalized to unit integrated area. The logarithm of the count is plotted. If the film were uniform in thickness and interconnectivity, the fluorescent intensity would be uniform and the histogram would show a single narrow spike.These histograms quantify the intensity variation to the limit of the optical resolution. Optical features such as bright spots of a few nanometers or less can be detected by fluorescence microscopy; but the spots cannot be resolved to less than the optical resolution.

Films prepared by the dilute vapor-phase deposition method showed the most compact intensity distribution, indicating that the microscale structure and thickness of these films was the most uniform. The histograms of films prepared from the concentrated vapor-phase deposition method and organic-phase deposition method show much wider intensity variation, suggesting that those films were less uniform than films prepared from aqueous and dilute vapor-phase deposition methods.

Accessible Amine Groups

Knowledge of the density of available reactive groups on a functionalized surface is important for many applications. Although cartoons of APTES functionalized glass often show a uniform monolayer, it is unlikely that such films exist. The amine group itself has a high affinity to the glass surface, (Vandenberg *et al*., 1991; White and Tripp, 2000; Kanan *et al*., 2002) so it is likely that many of the APTES molecules are oriented with the amine group on the glass. Furthermore, water catalyzes silane–silane bond formation, and trace amounts of water are present in either the solvent or adsorbed on the glass surface (Pantano, 1985). Therefore, it is likely that solution deposition results in the attachment of some prepolymerized assemblies. For many applications, particularly those in which the attached group is strongly charged (such as DNA and many proteins), it is important to cover the glass surface completely. This is true even at the expense of forming a multilayer film. The functionalized surface may consist of nonuniform, nonaligned regions, molecular voids, and multilayer islands. This lack of order may result in inaccessible amine groups, or in a film that contains defects, so that the amine accessibility varies with the molecular size of the reactive group. This "jumbled-structure" view of the reactive amine groups agrees with suggestions from previous studies of APTES/glass interactions (Vandenberg *et al*., 1991; White and Tripp, 2000; Kanan *et al*., 2002). We agree with the disordered film arrangement suggested by White and Tripp (2000), although our films were much thicker than the monolayers sketched there.

We evaluated the density and accessibility of the amino groups by reaction with either picric acid or with SPDP cross-linked RITC (SPDP–RITC). The picric acid method is an established spectrophotometric method to evaluate the amine density on the substrate surface. Primary amine groups on the film react with picric acid to form the colored picrate group, which is released from the surface into the solution. The density of amine groups is calculated from the characteristic absorption of picrate at 358 nm. Since the method involved separate reaction and elution steps with an intermediate rinsing of unreacted picric acid, elution of bound picrate did not expose unreacted amine groups to further reaction.

We developed a similar method that may provide a better measure of functionalizable amines. This method is based on SPDP, which is widely used in conjugating macromolecules with active amine or thiol groups (Ngo, 1986; Gaur and Gupta, 1989; Hermanson, 1999). The optical absorption of the released pyridine-2-thione group can be used to quantify the amount of SPDP cross-linked. However, for the surface coverage here, the pyridine-2-thione concentration was too low. Instead, we used SPDP cross-linked RITC to evaluate the exposed amine density. It may be possible to measure low amine-density directly by attaching an amine-reactive fluorophore (Nashat *et al*., 1998). However, such a technique will fail for most fluorophores, because of self-quenching at high concentration. Quenching by the surface is also possible, especially if the films are thin (Drexhage, 1970). By detaching the rhodamine, quenching can be overcome and the surface density determined from solution fluorescent intensity.

N-succinimidyl 3-[2-pyridyldithio]-propionamide molecules were fixed to the surface by reacting them with exposed amine groups. The free end of SPDP was then reacted with cystine to introduce a cleavable linker. Finally, the amine group was reacted with RITC, resulting in rhodamine attached to the surface through a cleavable cystine disulfide bond. This scheme is shown in Figure 1.

Although RITC reacts directly with exposed amine on the APTES film, it is difficult to quantitatively break the resulting thiourea bond and remove the rhodamine. This bond is reported to be easily hydrolyzed, (Banks and Paquette, 1995) but, at least for APTES conjugation, our experience suggests that it may be sterically protected. Removing directly attached RITC requires hydrolysis using a high concentration of NaOH at 80 °C, and under those conditions, much of the rhodamine is also destroyed. Milder hydrolysis using boiling water, or boiling aqueous solutions of triethanolamine or ethylenediamine leave considerable surface fluorescence. However with SPDP cross-linking, the attached rhodamine can be easily cleaved by reducing the disulfide bond with DTT, leaving little

residual fluorescence on the surface. Thus, the density of accessible APTES can be calculated from fluorescent intensity of the cleaved rhodamine in solution.

Figure 6 shows the density of reactive amines evaluated by the picric acid and the SPDP–RITC methods. The higher amine density from picrate may result from steric hindrance and entropic effects of the SPDP molecules, which are much larger than picric acid (trinitrophenol). It would be more difficult for SPDP molecules to react in regions where amine access depends on molecular- or nanoscale film defects. There may also be equilibrium and nonsteric kinetic differences between the reactions, Therefore, this method should be viewed as only semiquantitative. Figure 6 shows that vapor-phase deposition provides more accessible amine groups than the solution-based treatments. The molar ratio of reacted picrate to reacted SPDP–RITC was ~ 4 for concentrated and dilute vapor-phase deposition. The ratio was 2.2 and 6.5 for organic- and aqueous-phase deposition, respectively. The aqueous-phase deposition method produced the greatest difference in amine reactivity between picric acid and SPDP–RITC, which suggests heterogeneity in available amine. This method also produced the thinest and smoothest films (Figures 2–4).

The accessibility of the amino group on APTES surface is important for bioconjugation and macromolecular immobilization. The concentrated vapor-phase deposition method provides a high density of available amine groups (see Figure 6), but has many domains. Both dilute vapor-phase and aqueous-phase deposited films provide less amine reactivity, but a more uniform morphology. The organic-phase deposition produced the fewest SPDP/RITC-reactive groups, and it is the most nonuniform. Since the dilute vapor-phase deposition showed the most uniformity in both intrinsic and labeled fluorescence, it may be the best method for many applications.

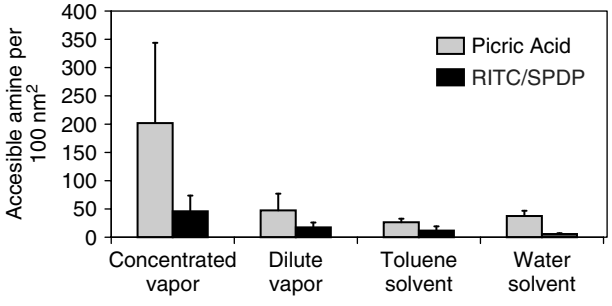

Fig 6. Accessible amine groups of (3-aminopropyl) triethoxysilane functionalized glass as measured by reaction with picric acid and with SPDP cross-linked rhodamine isothiocyanate. The differences in the ratio of SPDP–rhodamine cross-linked amine to the picrate available amine suggest differences in accessibility.

Atomic Force Microscopy Equivalent Optical Image

Insight to the chemical and physical structure of the films can be obtained from the optical equivalent of the AFM images. By the procedure outlined, see section on Methods, an estimate of the optical appearance of the film can be obtained in which the equivalent optical intensity is proportional to the physical AFM topography measurements. Therefore, the optical-equivalent image shows thick regions as bright spots. Figure 7 shows the optical equivalent of the AFM images of Figure 3, compared to gray-scale regions from the intrinsic and RITC-labeled optical images of Figures 2 and 4.

The optical equivalent AFM image (Figure 7A–E) shows many more domains in the vapor-phase deposition samples than shown by the optical images, suggesting that the fluorescent images do not capture the actual roughness of the sample. For the intrinsic fluorescence, this is understandable: most of the fluorescence is likely from the bulk film rather than the surface region. However, the RITC-labeled film should show similar roughness, since the image is of accessible amine that should be primarily on the surface. The expected intensity variation is not seen, and the histograms of Figure 5 suggest that the RITC-labeled intensity variation is even less than that of the intrinsic film. The lack of intensity variation, taken together with the large number of SPDP–RITC available amines and the low RITC fluorescent intensity (indicated by the long exposure time required) strongly suggest that the fluorescent features of the vapor-phase deposited layer are quenched by the high surface rhodamine density.

Atomic force microscopy and both fluorescent images show that the film deposited from the organic phase is rough and has many domains. Although there are domains both at the micro and nano scales (Figure 7C), and the domains are 5 to 10 times thicker than those of the vapor-phase deposition samples, the organic-phase deposited film has the fewest reactive amine groups and the least difference between picrate accessible and SPDP–RITC-accessible amines (see Figure 6). Taken together, these suggest a rough film with relatively few exposed amines. Such a film may be effective in rendering a glass surface inert but may be a poor choice for bioconjugation.

The aqueous-deposited film was the smoothest by both AFM and intrinsic fluorescence (Figure 7D). Atomic force microscopy measurements indicated a roughness similar to that of glass (data not shown). This smoothness, in view of the grainy appearance of the RITC-labeled image suggests film defects at the submicron level, possibly resulting from film rearrangement (Sun *et al*., 2002) or density changes during annealing. There was also a large difference in the ratio of picrate and SPDP–RITC-accessible amines (see Figure 6), which further suggests the presence

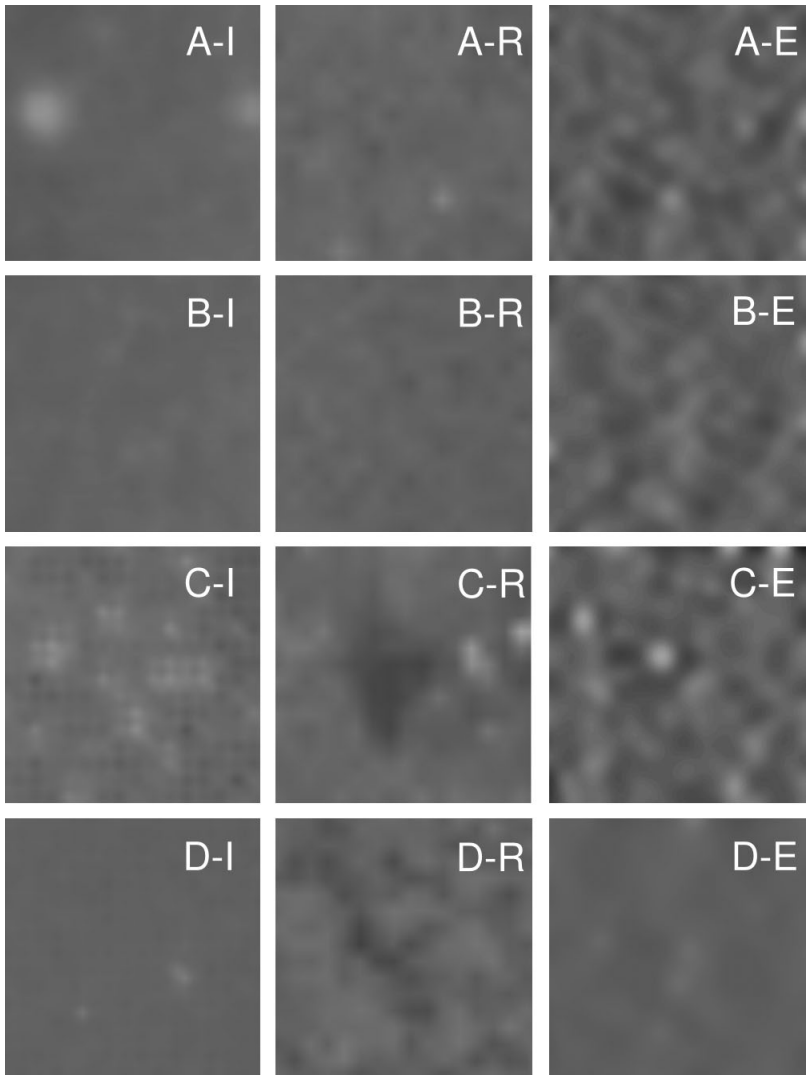

Fig 7. Optical equivalent appearance of the AFM images, assuming optical brightness is proportional to feature height. The equivalent optical image of h 5 μm square AFM scans, Figure 3, is compared with 5 μm square samples of fluorescent images for the intrinsic and (3-aminopropyl) triethoxysilane fluorescence surfaces from Figures 2 and 4. The panels from top to bottom are (A) concentrated vapor-phase deposition, (B) dilute vapor-phase deposition, (C) organic-phase deposition, and (D) aqueous-phase deposition. For each image, the label (I) indicates intrinsic fluorescence, (R) rhodamine-tagged fluorescence, or (E) equivalence optical appearance of the AFM topology. Intensity and contrast of the equivalent image were scaled to that of the normalized optical images.

of molecular or nanoscale features that affect amine accessiblity to SPDP–RITC. Individual nanoscale features that bind RITC can be resolved with optical microscopy if the features are separated by distances greater than the optical resolution. Therefore, molecular or nanoscale defects such as fissures or surface defects induced by density changes during annealing will be distinguishable if their spacing is sufficiently large.

Why Different Treatments Produce Different Properties

Our results show substantial differences in the morphology and reactivity of APTES films deposited by different methods. In this section, we propose mechanisms to explain these differences. We suggest that the differences between films produced by different deposition methods depends on the interaction of the film and retained solvent (or lack of solvent) during the annealing process, and the tendency for the inter-APTES reaction to form siloxane cross-links (Crampton *et al*., 2005; Howarter and Youngblood, 2006, 2007).

Both the amine and the triethoxy groups of the APTES show affinity to glass (Vandenberg *et al*., 1991; White and Tripp, 2000; Kanan *et al*., 2002). Furthermore, APTES is a small molecule so there is little tendency for alkyl chain interactions to induce film order, such as that seen in OTS. Together these suggest that

the initial deposition of the APTES film is disordered. If a solvent such as water or toluene is present, the lower density provides space for solvent entrapment in the deposited film. We view this solvent entrapment as similar to that occurring in thin spun-cast polymer films, where retained solvent can alter the mobility and properties of the polymers (Richardson *et al*., 2003). Furthermore, in spun-cast films the mole fraction of the retained solvent increases as the film thickness decreases into the nanometer range (Garcia-Turiel and Jerome, 2007), so the thickness of the deposited film will affect the fraction of solvent retrained.

The aqueous-deposited film was thin, as indicated by low intrinsic fluorescence (Figure 2) and featureless AFM measurements. (Figure 3) During annealing, some of the APTES will react with glass silanols, inducing order in the film that lasts over several layers. The ethoxy groups of unreacted APTES will tend to the air–film interface to avoid the hydrophobic environment of the propyl chains in the interior of the film. At the surface, intra-APTES siloxane bonds form. This molecular rearrangement of silanol during annealing will render many amines inaccessible. Also, the film density will increase during annealing, as entrained water is baked out. As the thin film becomes more dense, it shrinks and fissures and cracks will develop, exposing some buried amines to sufficiently small amine-reactive groups. These processes will result in a smooth film that shows nanoscale defects and a preference for smaller amine-reactive groups. Small nanoscale fissures and defects would not have shown on AFM scans at our lateral resolution. However if some defects are large enough to allow RITC penetration, an image like that seen in Figure 4(D) will be expected.

The organic-phase deposited films appeared relatively thick, from our intrinsic fluorescence measurements (Figure 2) and they had the largest island peaks, as measured by AFM (Figure 4). As films annealed, the ethoxy groups would rearrange to the glass and air surfaces to avoid the strongly hydrophobic toluene–propyl chain interior of the film. Intra-APTES siloxane cross-links would form in the regions of high siloxane density. Since these films were thick there would be less substrate-induced order but solvent would still be available to facilitate mobility. Islands formed in past studies of annealing (Sun *et al*., 2002; Crampton *et al*., 2006), and the large islands shown by our imaging techniques support the idea that silane molecules are mobile. When the film is sufficiently thick it can cross-link without forming fissures or defects. Therefore, the annealed film would be rough film with a high density of ethoxy groups at the air–film interface and little difference between picrate and SPDP–RITC reactivity.

The concentrated and dilute vapor-phase deposited films did not have entrained solvent, so they would be less mobile during annealing and more likely to form inter-APTES cross-links in place. Amines at the air–film interface would be less likely to be displaced by migrating ethoxy groups and would remain accessible. This reduced mobility of APTES is suggested by the small, regular island formation shown in Figure 3(A) and (B). The concentrated vapor-phase film was thicker, so the APTES mobility would be less constrained by order induced by the glass surface, than the dilute vapor-phase deposited film. Therefore, the concentrated vapor-phase film would have larger islands, though in both cases more amine groups will be accessible than for solvent deposited films.

Conclusions

In summary, there were considerable differences in the morphology and accessibility of APTES films prepared from the four methods. We suggest that these differences are the result of film thickness and the differences in the mobility of the APTES during the annealing process. Films prepared by dilute vapor-phase deposition were the most uniform and had many available reactive amines. Films prepared from the concentrate vapor-phase deposition method appeared to be the thickest and had the most accessible amine groups. Films prepared by organic-phase deposition were thick, rough, and relatively inert. Films prepared by aqueous deposition were thin and smooth, but did not have a high density of reactive amine available to larger molecules. For bioconjugation or macromolecule immobilization applications, dilute vapor-phase deposition method produced APTES films that were uniform and had a high density of accessible amino groups.

Acknowledgement

Support from National Science Foundation grant 0134594 is gratefully acknowledged.

References

Allen G, Sorbello F, Altavilla C, Castorina A, Ciliberto E: Macro-, micro- and nano-investigations on 3-aminopropyl trimethoxysilane self-assembly-monolayers. *Thin Solid Films* **483**, 306–311 (2005).

Banks PR, Paquette DM: Comparison of 3 common amine reactive fluorescent-probes used for conjugation to biomolecules by capillary zone electrophoresis. *Bioconjug Chem* **6**, 447–458 (1995).

Bekiari V, Lianos P: Characterization of photoluminescence from a material made by interaction of (3-aminopropyl)triethoxysilane with acetic acid. *Langmuir* **14**, 3459–3461 (1998).

Benitez JJ, Ogletree DF, Salmeron M: Preparation and characterization of self-assembled multilayers of octadecylamine on mica from ethanol solutions. *Langmuir* **19**, 3276–3281 (2003).

Born M, Wolf E: *Principles of Optics*, Cambridge University Press, Cambridge (1980).

Chechik V, Stirling CJM: Reactivity in self-assembled monolayers, effect of the distance from the reaction center to the monolayer-solution interface. *Langmuir* **14**, 99–105 (1998).

Chen QZ, Rezwan K, Armitage D, Nazhat SN, Boccaccini AR: The surface functionalization of 45s5 bioglass (r)-based glass-ceramic scaffolds and its impact on bioactivity. *J Mater Sci Mater Med* **17**, 979–987 (2006).

Crampton N, Bonass WA, Kirkham J, Thomson NH: Formation of aminosilane-functionalized mica for atomic force microscopy imaging of DNA. *Langmuir* **21**, 7884–7891 (2005).

Crampton N, Bonass WA, Kirkham J, Thomson NH: Studying silane mobility on hydrated mica using ambient AFM. *Ultramicroscopy* **106**, 765–770 (2006).

Drexhage KH: Influence of a dielectric interface on fluorescence decay time. *J Luminescence* **1–2**, 693 (1970).

Ek S, Iiskola EI, Niinisto L: Gas-phase deposition of aminopropylalkoxysilanes on porous silica. *Langmuir* **19**, 3461–3471 (2003).

Enders D, Nagao T, Nakayama T, Aono M: In situ surface-enhanced infrared absorption spectroscopy for the analysis of the adsorption and desorption process of au nanoparticles on the SiO_2/Si surface. *Langmuir* **23**, 6119–6125 (2007).

Etienne M, Walcarius A: Analytical investigation of the chemical reactivity and stability of aminopropyl-grafted silica in aqueous medium. *Talanta* **59**, 1173–1188 (2003).

Falsey JR, Renil M, Park S, Li SJ, Lam KS: Peptide and small molecule microarray for high throughput cell adhesion and functional assays. *Bioconjug Chem* **12**, 346–353 (2001).

Fan FQ, Maldarelli C, Couzis A: Fabrication of surfaces with nanoislands of chemical functionality by the phase separation of self-assembling monolayers on silicon. *Langmuir* **19**, 3254–3265 (2003).

Foisner J, Glaser A, Kattner J, Hoffmann H, Friedbacher G: Atomic force microscopy investigation of the growth of different alkylsiloxane monolayers from highly concentrated solutions. *Langmuir* **19**, 3741–3746 (2003).

Frey A, Neutra MR, Robey FA: Peptomer aluminum oxide nanoparticle conjugates as systemic and mucosal vaccine candidates: synthesis and characterization of a conjugate derived from the C4 domain of HIV-1 (MN) gp120. *Bioconjug Chem* **8**, 424–433 (1997).

Garcia-Turiel J, Jerome B: Solvent retention in thin polymer films studied by gas chromatography. *Colloid Polym Sci* **285**, 1617–1623 (2007).

Gaur RK, Gupta KC: A spectrophotometric method for the estimation of amino-groups on polymer supports. *Anal Biochem* **180**, 253–258 (1989).

Gisin BF: The monitoring of reactions in solid-phase peptide synthesis with picric acid. *Anal Chim Acta* **58**, 248–249 (1972).

Gyorvary E, Wetzer B, Sleytr UB, Sinner A, Offenhausser A, *et al*.: Lateral diffusion of lipids in silane-, dextran-, and s-layer-supported mono- and bilayers. *Langmuir* **15**, 1337–1347 (1999).

Heiney P, Gruneberg K, Fang J, Dulcey C, Shashidhar R: Structure and growth of chromophore-functionalized (3-aminopropyl)triethoxysilane self-assembled on silicon. *Langmuir* **16**, 2651–2657 (2000).

Hermanson GT: *Bioconjugate Techniques*, Academic Press, New York (1999).

Howarter JA, Youngblood JP: Optimization of silica silanization by 3-aminopropyl triethoxysilane. *Langmuir* **22**, 11142–11147 (2006).

Howarter JA, Youngblood JP: Surface modification of polymers with 3-aminopropy ltriethoxysilane as a general pretreatment for controlled wettability. *Macromolecules* **40**, 1128–1132 (2007).

Hu J, Wang M, Weier HUG, Frantz P, Kolbe W, *et al*.: Imaging of single extended DNA molecules on flat (aminopropyl)triethoxysilane-mica by atomic force microscopy. *Langmuir* **12**, 1697–1700 (1996).

Jin L, Horgan A, Levicky R: Preparation of end-tethered DNA monolayers on siliceous surfaces using heterobifunctional cross-linkers. *Langmuir* **19**, 6968–6975 (2003).

Joos B, Kuster H, Cone R: Covalent attachment of hybridizable oligonucleotides to glass supports. *Anal Biochem* **247**, 96–101 (1997).

Jung GY, Li ZY, Wu W, Chen Y, Olynick DL, *et al*.: Vapor-phase self-assembled monolayer for improved mold release in nanoimprint lithography. *Langmuir* **21**, 1158–1161 (2005).

Kanan SA, Tze WTY, Tripp CP: Method to double the surface concentration and control the orientation of adsorbed (3-aminopropyl)dimethylethoxysilane on silica powders and glass slides. *Langmuir* **18**, 6623–6627 (2002).

Kang HJ, Blum FD: Structure and dynamics of amino functional silanes adorbed on silica surfaces. *J Phys Chem* **95**, 9391–9396 (1991).

Keller H: Objective lenses for confocal microscopy. In *Handbook of Biological Confocal Microscopy*, (Ed. Pawley J), Springer Science+Business, New York, 145–161 (2006).

Kessel CR, Granick S: Formation and characterization of a highly ordered and well-anchored alkylsilane monolayer on mica by self-assembly. *Langmuir* **7**, 532–538 (1991).

Kim SR, Abbott NL: Manipulation of the orientational response of liquid crystals to proteins specifically bound to covalently immobilized and mechanically sheared films of functionalized bovine serum albumin. *Langmuir* **18**, 5269–5276 (2002).

Koga T, Morita M, Ishida H, Yakabe H, Sasaki S, *et al*.: Dependence of the molecular aggregation state of octadecylsiloxane monolayers on preparation methods. *Langmuir* **21**, 905–910 (2005).

Kurth DG, Bein T: Surface reactions on thin layers of silane coupling agents. *Langmuir* **9**, 2965–2973 (1993).

Kurth DG, Bein T: Thin-films of (3-aminopropyl)triethoxysilane on aluminum-oxide and gold substrates. *Langmuir* **11**, 3061–3067 (1995).

Legrange JD, Markham JL, Kurkjian CR: Effects of surface hydration on the deposition of silane monolayers on silica. *Langmuir* **9**, 1749–1753 (1993).

LeProust E, Zhang H, Yu PL, Zhou XC, Gao XL: Characterization of oligodeoxyribonucleotide synthesis on glass plates. *Nucleic Acids Res* **29**, 2171–2180 (2001).

Macdonald RI: Characteristics of self-quenching of the fluorescence of lipid-conjugated rhodamine in membranes. *J Biol Chem* **265**, 13533–13539 (1990).

Martin HJ, Schulz KH, Bumgardner JD, Walters KB: XPS study on the use of 3-aminopropyltriethoxysilane to bond chitosan to a titanium surface. *Langmuir* **23**, 6645–6651 (2007).

Matsumoto A, Tsutsumi K, Schumacher K, Unger KK: Surface functionalization and stabilization of mesoporous silica spheres by silanization and their adsorption characteristics. *Langmuir* **18**, 4014–4019 (2002).

McGovern ME, Kallury KMR, Thompson M: Role of solvent on the silanization of glass with octadecyltrichlorosilane. *Langmuir* **10**, 3607–3614 (1994).

Metwalli E, Haines D, Becker O, Conzone S, Pantano C: Surface characterizations of mono-, di-, and tri-aminosilane treated glass substrates. *J Colloid Interface Sci* **298**, 825–831 (2006).

Miyazaki M, Kaneno J, Uehara M, Fujii M, Shimizu H, *et al*.: Simple method for preparation of nanostructure

on microchannel surface and its usage for enzyme-immobilization. *Chem Commun*, (5), 648–649 (2003).

Moon JH, Shin JW, Kim SY, Park JW: Formation of uniform aminosilane thin layers: an imine formation to measure relative surface density of the amine group. *Langmuir* **12**, 4621–4624 (1996).

Moon JH, Kim JH, Kim K, Kang TH, Kim B, *et al*.: Absolute surface density of the amine group of the aminosilylated thin layers: ultraviolet-visible spectroscopy, second harmonic generation, and synchrotron-radiation photoelectron spectroscopy study. *Langmuir* **13**, 4305–4310 (1997).

Nakagawa T, Ogawa K, Kurumizawa T: Atomic-force microscope images of monolayers from alkyltrichlorosilane on mica surfaces and studies on an anchoring mechanism of alkyltrichlorosilane molecules to the surface. *Langmuir* **10**, 525–529 (1994).

Nashat AH, Moronne M, Ferrari M: Detection of functional groups and antibodies on microfabricated surfaces by confocal microscopy. *Biotechnol Bioeng* **60**, 137–146 (1998).

Ngo TT: A simple spectrophotometric determination of solid supported amino-groups. *J Biochem Biophys Methods* **12**, 349–354 (1986).

Pantano CG. Surface chemistry in relation to the strength and fracture of silicate glasses. In *Strength of Inorganic Glass*, (Ed. Kurkjian CR). Plenum Press: New York, 37–66 (1985).

Peanasky J, Schneider HM, Granick S, Kessel CR: Self-assembled monolayers on mica for experiments utilizing the surface forces apparatus. *Langmuir* **11**, 953–962 (1995).

Peters RD, Nealey PF, Crain JN, Himpsel FJ: A near edge x-ray absorption fine structure spectroscopy investigation of the structure of self-assembled films of octadecyltrichlorosilane. *Langmuir* **18**, 1250–1256 (2002).

Rasband WS, Image J. U. S. National Institutes of Health, Bethesda, Maryland, http://rsb.info.nih.gov/ij/, (1997–2007).

Richardson H, Sferrazza M, Keddie JL: Influence of the glass transition on solvent loss from spin-cast glassy polymer thin films. *Eur Phys J E* **12**, S87–S91 (2003).

Rozlosnik N, Gerstenberg MC, Larsen NB: Effect of solvents and concentration on the formation of a self-assembled monolayer of octadecylsiloxane on silicon (001). *Langmuir* **19**, 1182–1188 (2003).

Simon A, Cohen-Bouhacina T, Porte M, Aime J, Baquey C: Study of two grafting methods for obtaining a 3-aminopropyltriethoxysilane monolayer on silica surface. *J Colloid Interface Sci* **251**, 278–283 (2002).

Stevens MJ: Thoughts on the structure of alkylsilane monolayers. *Langmuir* **15**, 2773–2778 (1999).

Sun CH, Aston DE, Berg JC: Structural evolution of octyltriethoxysilane films on glass surfaces during annealing at elevated temperature. *J Colloid Interface Sci* **248**, 96–102 (2002).

Szabo A, Gournis D, Karakassides MA, Petridis D: Clay-aminopropylsiloxane compositions. *Chem Mater* **10**, 639–645 (1998).

Tidswell IM, Rabedeau TA, Pershan PS, Kosowsky S, Folkers JP, *et al*.: X-ray grazing-incidence diffraction from alkylsiloxane monolayers on silicon-wafers. *J Chem Phys* **95**, 2854–2861 (1991).

Uchida Y, Nobu YI, Momiji I, Matsui K: Luminescence of silica-pillared clays and gels derived from aminofunctional silanes. *J Sol-Gel Sci Technol* **19**, 705–709 (2000).

Ulman A: Formation and structure of self-assembled monolayers. *Chem Rev* **96**, 1533–1554 (1996).

Vaidya AA, Norton ML: DNA attachment chemistry at the flexible silicone elastomer surface: toward disposable microarrays. *Langmuir* **20**, 11100–11107 (2004).

Vandenberg E, Bertilsson L, Liedberg B, Uvdal K, Erlandsson R, *et al*.: Structure of 3-aminopropyl triethoxy silane on silicon oxide. *J Colloid Interface Sci* **147**, 103–118 (1991).

Waddell TG, Leyden DE, Debello MT: The nature of organosilane to silica-surface bonding. *J Am Chem Soc* **103**, 5303–5307 (1981).

Wang YL, Lieberman M: Growth of ultrasmooth octadecyltrichlorosilane self-assembled monolayers on SIO_2. *Langmuir* **19**, 1159–1167 (2003).

Wang B, Abdulali-Kanji Z, Dodwell E, Horton JH, Oleschuk RD: Surface characterization using chemical force microscopy and the flow performance of modified polydimethylsiloxane for microfluidic device applications. *Electrophoresis* **24**, 1442–1450 (2003).

White LD, Tripp CP: Reaction of (3-aminopropyl)dimethylethoxysilane with amine catalysts on silica surfaces. *J Colloid Interface Sci* **232**, 400–407 (2000).

Wikstrom P, Mandenius CF, Larsson PO: Gas-phase silylation, a rapid method for preparation of high-performance liquid-chromatography supports. *J Chromatogr* **455**, 105–117 (1988).

Xiao XD, Liu GY, Charych DH, Salmeron M: Preparation, structure, and mechanical stability of alkylsilane monolayers on mica. *Langmuir* **11**, 1600–1604 (1995).

Yu L, Li CM, Zhou Q, Gan Y, Bao QL: Functionalized multi-walled carbon nanotubes as affinity ligands. *Nanotechnology* **18**, 116614 (2007).

Zhang FX, Srinivasan MP: Self-assembled molecular films of aminosilanes and their immobilization capacities. *Langmuir* **20**, 2309–2314 (2004).

Zhuang XW, Ha T, Kim HD, Centner T, Labeit S, *et al*.: Fluorescence quenching: a tool for single-molecule protein-folding study. *Proc Natl Acad Sci USA* **97**, 14241–14244 (2000).